Enhancement of Adhesive Joint Strength by Surface Texturing

W. V. CHANG, *Department of Chemical Engineering, University of Southern California, Los Angeles, California 90007*, and J. S. WANG, *Department of Electrical Engineering, University of Southern California, Los Angeles, California 90007*

Synopsis

Proper substrate preparation is an indispensible step for achieving strong adhesive joints. One consequence of such surface treatment is the enhancement of degree of mechanical interlocking between polymers and substrates, which, according to the literature, seems to increase the strength of the joint. A novel method based on photolithography is developed to texture aluminum oxide surface by controlling the pit size and its spatial distribution. Surface profile, surface physical chemical properties of this sample, and the lap shear strength of epoxy adhesive joints are compared with those of the phosphoric acid anodized (PAA) sample. It is shown that the lap shear strength of the textured sample is superior to that of the PAA sample. Surface profile data and mathematical analysis suggest that the inferiority of the PAA sample is probably due to the trapped air in the large pit in the surface resisting the penetration of adhesives. It also concludes that the high surface area provided by the multitude small pits in PAA sample is far from being fully utilized. This study opens up a new avenue to rationally improve the strength of adhesive joint by controlling the surface profile, the surface chemical properties, and the pressure during bond formation.

INTRODUCTION

One rapidly and steadily growing area in the polymer field is adhesives technology. During the past decade, industrial growth in adhesives has consistently outstripped the general economy with an average annual growth in tonnage of about 7%.[1] This increase, however, is small compared to the potential of adhesives, and a major factor restricting growth is the lack of confidence of design engineers in predicting the strength of adhesive joints from a knowledge of the properties of the adherend and the adhesive. A direct consequence of this unsatisfactory situation is that extensive and costly engineering development efforts must be undertaken to qualify a unique adhesive system for a given application.[2]

Several theories such as chemical adsorption theory,[3] electrostatic theory,[4] diffusion theory,[5] acid–base interaction,[2,6] and surface energetics and wetting theories[7,8] have been proposed to relate the strength of adhesive joint to the molecular properties of the two surfaces in contact during bond formation. Many attempts have also been directed to correlate adhesive joint strength values to different surface chemical criteria (for a recent one, please see Ref. 9). Without doubt, interfacial thermodynamic properties affect greatly the performance of an adhesive joint; however, the latter also depends greatly on the exact way that the bond is formed. As has been pointed out by Bikerman[10] and Schonhorn,[11] adhesion (the interfacial phenomenon) and adhesive joint strength are two distinctly different concepts; and, hence, the mechanical failure of a joint in

Journal of Applied Polymer Science, Vol. 26, 1759–1776 (1981)
 CCC 0021-8995/81/061759-18$01.80

general reveals nothing directly about interfacial forces. Without more detailed information on the morphology of adhesives at the interface, any apparent success of a correlation between the interfacial thermodynamical properties and joint strength has only dubious value.

From the continuum-mechanics point of view, the strength of adhesive joints depends only on the loading history of the system and the constitutive equations of the adhesive, the adherend, and the adhesive–adherend interface. For a given time scale, the most important material parameters are the characteristic fracture energy and flaw size of both the adhesive and the adherend and the adhesive fracture energy and flaw size of the interface.[12,13]

The prerequisites for a strong durable bond are sufficient contact between adhesives and adherends and the removal from the interface of all traces of solid, liquid, or vapor having weaker cohesive strength than the adhesive and adherend. In order to obtain sufficient contact, an adhesive has to be applied in the liquid state. The degree of contact depends on the viscosity of the liquid adhesives, the wettability[14,15] of adherends, the surface roughness, and the time allowed for bond formation. Pretreatment of adherend surfaces will change both the wettability and the surface roughness of adherends and, hence, will affect the degree of surface contact. Proper substrate preparation will also remove low-strength impurities from the adherend surface.

Surface preparation is a highly developed art. Information can be found in many papers and commercial technical bulletins, but unfortunately very few systematic comparisons of various treatments exist. As a consequence of our lack of scientific understanding, we know only that a particular treatment of a given adherend–adhesive system is beneficial, but we do not know whether the same treatment is valid for a different system.

In order to unveil the mystery surrounding surface preparation techniques, it is desirable (maybe even indispensable) to prepare a model surface of which some surface properties can be well controlled. One of those properties is surface profile. In a recent study by Oliver and Mason[16] of the effect of surface roughness on the spreading behavior of liquids, the surface was textured by mechanical cutting, which limited the type and the size of surface pattern that could be introduced.

In this report we would like to introduce a new surface preparation technique which is based on photolithography.[17] This technique has the potential of introducing pores down to the size of μm range into the surface. The aluminum–epoxy system was chosen for the study because abundant information of the systems is available in the literature. Joint strength of the system treated by this technique is measured and compared with the conventional PAA (phosphoric acid anodize) specimen.

EXPERIMENTAL

Materials

Adherends. The adherends used were 7075-T6 aluminum panels with a thickness of 0.0032 m (0.125 in.), all in the bare condition.

Adhesive and primers. Two systems, one being 121°C (250°F) cure and the other 177°C (350°F) cure, are used. The former consists of the FM 123-2 ad-

hesive and the BR 127 corrosion inhibiting primer, both of which were supplied by the American Cynamid Co., Bloomingdale Dept., Havre de Grace, Md. FM-123-2 adhesive is a modified nitrile epoxy adhesive manufactured as a supported film of a 0.028-cm-thick on a nonwoven Dacron mat carrier. BR-127 is a modified epoxy-phenolic adhesive primer. The high-temperature system which consists of the PL 729-3 adhesive and PL 728 corrosion inhibiting primer was supplied by the BFGoodrich Co., Adhesive Products Division, Akron, Ohio. PL 729-3 is a modified film epoxy adhesive which has a nylon tricot carrier and an areal density of 0.488 kg/m^2.

Phosphoric Acid Anodize

Cleaning. Aluminum panels of dimensions 0.152 × 0.152 × 0.0032 m (6 × 6 × 0.125 in.) were vapor degreased in trichloroethylene and then immersed for 10 min at a temperature of 79°C in the alkaline cleaning solution consisting of 60.0 kg/m^3 Oaklite #164 in distilled water. Panels were then immersed and rinsed in flowing tap water at room temperature for 10 min. Panels were subsequently immersed in the deoxidizer solution for 2 min at room temperature, followed by an immersion rinse in flowing tap water at room temperature for 10 min. The deoxidizer solution consisted of 120 kg/m^3 Oaklite #34 and 18.75 kg/m^3 sulfuric acid in distilled water.

Anodizing. Panels were phosphoric acid anodized at room temperature in the electrolyte consisting of a solution of 10% by weight phosphoric acid in distilled water. The voltage was gradually increased from 0 to 10 V over a period of 1 min and maintained at 10 V for 22 min. Panels were then immersion rinsed in flowing tap water for 15 min, followed by forced air drying at 66°C.

Surface Texturing by Photolithography

This technique, which is borrowed from the well-established semiconductor device technology, consists of two major jobs: (1) photographic mask making and (2) photochemical etching.

Photographic mask making. Mask making begins with a large-scale layout called artwork. The artwork was made 50 times as larger as the final size to avoid large errors and to be of size reasonable for human operations. A MicroPlotter Linear Coordinatograph is used to guide a very sharp knife blade in the XY-plane. Attachments are available for circular cuts. Layout was done on a plastic material called Rubylith, a clean Mylar with red plastic coating. Cuts are made in the red coating, and the coating is peeled off in the appropriate region. In this work, two lines of 50 circles were drawn, the diameter being 2.5 mm and edge-to-edge distance between nearest circles being 7.5 mm. The artwork is then photographed by a Microkon Reduction Camera to be reduced to 1/50 of its original size; i.e., the diameter of the circles is now 50 μmm. This mask will be used in the photoresist operation to transfer the layout pattern to the aluminum surface. Because a large number of patterns in the desired area a 2 × 2 cm, the multiple images of the initial layout were produced by the use of a computer-aided control to move the focus and the shutter automatically.

Photochemical etching. Aluminum panels were first cut into specimens of 4 × 2 × 0.32 cm and then subjected to three additional processing steps: cleaning, photoresist processing, and etching.

(a) *Cleaning.* Specimens were immersed in trichloroethylene at 80°C for 10 min, then in acetone at room temperature for 5 min, and rinsed in deionized water. Specimens cleaned by the above method were followed by a more effective alkaline cleaning. Because aluminum is readily attacked by alkaline solution, nonetching cleaner was used to inhibit or to minimize the attack on the aluminum surface. Specimens were immersed in nonetching solution at 60–70°C for 5 min, then rinsed in warm water, and dried in nitrogen flow. The nonetching solution consisted of 21 g sodium carbonate and 21 g sodium metasilicate per 4 dm^3 water.

(b) *Photoresist processing.* The photoresist serves two main functions, namely, to be capable of reproducing the photomask pattern with a high degree of accuracy and to provide satisfying masking of coated surface for subsequent etching. The procedure is as follows: (1) Place specimens on spinner chuck and vacuum the system. (2) Apply photoresist to cover entire surface, photoresist being 1 volume Kodak Micro-Resist-752 diluted with 1 volume Kodak Micro Resist Thinner. (3) Start spin cycle and spin 20 sec at 3600 rpm to produce a uniform resist film of thickness 1–2 μm. (4) Repeat (2) and (3) for second coat. (5) Prebake the resist coating in an oven at 85°C for 10 min. (6) Place on the vacuum chuck of the alignment fixture and align to proper mask. (7) Expose the resist coating with high-pressure mercury vapor lamp for 15 sec. (8) Develop the resist image by immersing in Kodak Micro Resist Developer for 3 min. (9) Rinse the resist image with Kodak Micro Resist Rinse immediately after development for 1 min. (10) Dry the resist image in dry nitrogen. (11) Postbake the resist image in an oven at 120°C for 1 hr.

(c) *Chemical Etching.* Chemical etching is the removal of material by dissolution or chemical reaction in suitable etchant. Photoresist must be able to resist the etchant. (1) Etch exposed aluminum surface by immersing Aluminum Etchant (Transene Co., Rowley, Mass.) at 50°C for 20 min with constant stirring. Etching time should be kept within 25 min, otherwise the photoresist pattern would be broken down and be lifted off. (3) Rinse in deionized water. (4) Remove photoresist by immersing in IRC Laboratory J-100 Stripper 95°C for 10 min. (5) Dry in nitrogen flow.

Surface Texture

The surface texture of both PAA specimens and photolithographically textured specimens were examined with a microscope and a Dektak Surface Profile Measuring System.

Surface Physical Chemical Properties

The tools that were used to characterize the surface were ellipsometry, which monitors film thickness, refractive index and surface roughness; surface potential difference (SPD), which reveals film dielectric properties; photoelectron emission (PEE), which reveals electron emission and attenuation properties; and surface energetics (SE), as measured by liquid drop contact angles.[18,19] Experiments were conducted at Rockwell International Science Center by Dr. T. Smith. A description of the experimental techniques is given in Ref. 18.

Mechanical Testing

Due to the size limitation imposed by our photoresist process, the size of the specimens used for the lap shear test is only 4 × 2 × 0.32 cm, which is not the standard ASTM size. Bare aluminum specimens and those treated by PAA or photolithographic texturing were first subjected to solvent cleaning before the adhesives were applied.

Solvent cleaning. Solvent cleaning consists of the following steps: (1) immersion and brush cleaning in trichloroethylene at 80°C for 10 min; (2) immersion in acetone at room temperature for 5 min; (3) immersion in methanol for 5 min at room temperature; (4) drying in air at room temperature.

Primer application. Primer was allowed to warm to room temperature prior to opening the container and was, thoroughly mixed before and agitated during application. Both primers were brushed and air dried for at least 30 min to a dry primer thickness of 5 μm. They were then cured in an oven and isolated from dust by aluminum foil cover, at 121°C, 30 min, for PL728 and 60 min for BR127.

Bonding procedure. Adhesive rolls were allowed to warm to room temperature before unrolling and were cut into patterns of 2 × 2 cm squares, which were then applied to the aluminum surface. Specimens were then subjected to compression pressure imposed by a press. Temperature was then brought up to the desired value in 30 min. The specimens were in the press for 60 min, during which the pressure was kept constant. Supporting aluminum plates of the same thickness were used in order to apply a uniform compression (to avoid bending) to the specimens.

Lap shear tests. Tests were conducted on an Instron tester at room temperature, at a pull speed of 84.7 μm/sec. Care was taken to avoid specimen slippage from the grips and to avoid imposing bending action on the specimens. Some specimens were immersed in water for 100 days before lap shear testing in order to investigate the environmental effect.

RESULTS

Pore distribution in a photolithographically textured specimen is given in Figure 1, which shows a rather uniform spatial distribution, indicating the success of this technique. Surface profiles of bare, PAA, and textured aluminum are given in Figures 2, 3, and 4, respectively. These figures reveal the depth distribution of holes and diameter distribution of opening windows. The depth of holes ranges from 8 to 13 μm, with about 60% of them being larger than 10 μm and the rest less than 10 μm. The diameter of opening windows can also be measured by microscopy, which indicates diameter ranges from 70 to 90 μm, with 40% being about 70 μm, 20% about 90 μm, and the rest falling in between.

The typical surface profile of bare aluminum is very irregular, with many sharp spikes protruding from the surface, which may act as stress concentrators in an adhesive bond and hence weaken the joint. PAA surface is more regular, but some spikes still exist. Textured surface not only has the most regular structure but also the deepest holes in the surface, providing the largest surface area without introducing stress concentrators.

Undercutting, which is a constant problem in integrated circuit board technology, is also a potential problem here, as indicated by the window size (70–90

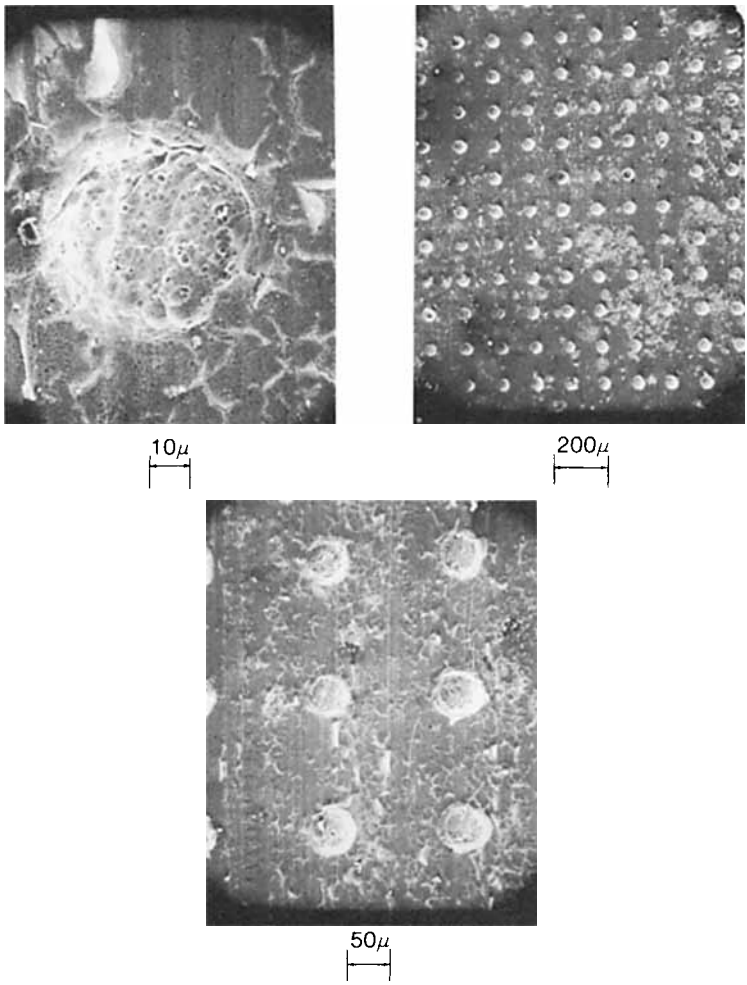

Fig. 1. Pore size and its distribution in a textured specimen.

μm) being larger than the design value (50 μm). The etch factor, as defined in Figure 5, is about 1, which is acceptable according to the standard of solid-state industry. Although the etch factor can be increased by many techniques such as conversion coating, it is not clear if such an improvement is necessary for our course.

Data of lap shear strength are given in Tables I–III. The mean and the standard deviation of each test condition are calculated based on a sample size of 6 to 10 specimens. Lap shear joint strength in our study is strikingly lower than that of a typical PAA specimen. This is probably due to the differences in both the bond formation condition and the size of specimens used in our study and those used in the standard ASTM method.

Surface properties of aluminum samples are presented in Table IV.

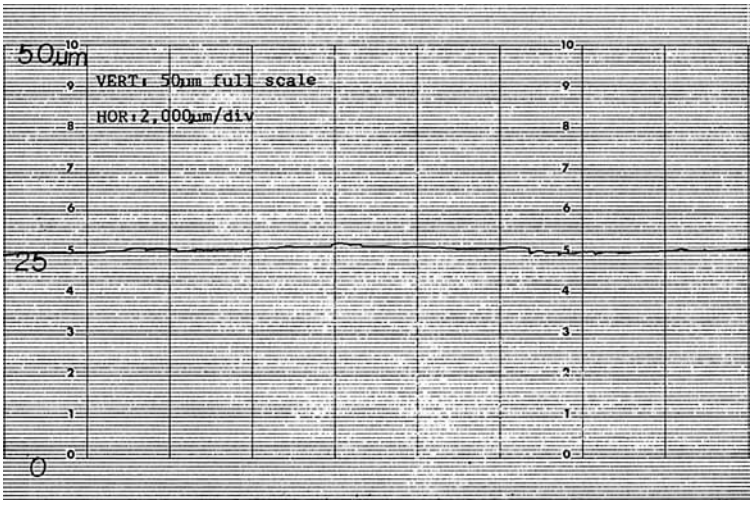

(a)

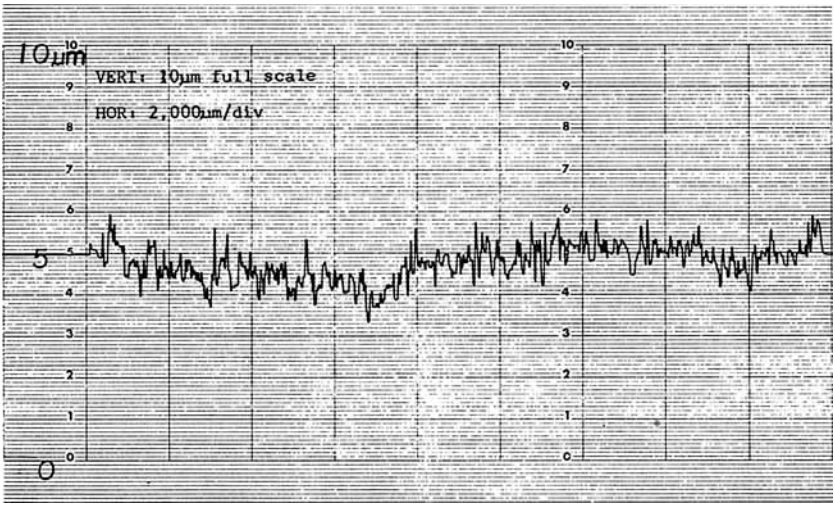

(b)

Fig. 2. Surface profile recording of bare aluminum.

DISCUSSIONS

Due to its relevance to the aerospace industry, surface treatment of aluminum has received considerable attention. Three methods—PAA (phosphoric acid anodize), FPL (Forest Products Laboratory), and CAA (chromic acid anodize)—have been widely used, among which PAA seems to display the most superior performance. Its superiority may be of both physical (or morphological) and chemical origins; however, experimental data[18,20,21] seem to suggest that the former is the dominant one. The idealized surface textures of aluminum treated by FPL, PAA, and CAA are schematically presented in Figures 6, 7, and 8, respectively (reproduced from Ref. 2). The striking feature of the PAA surface is its highly porous and thick oxide film which provides a very large surface area. The porous open structure and the polar nature of the outer surface (covered

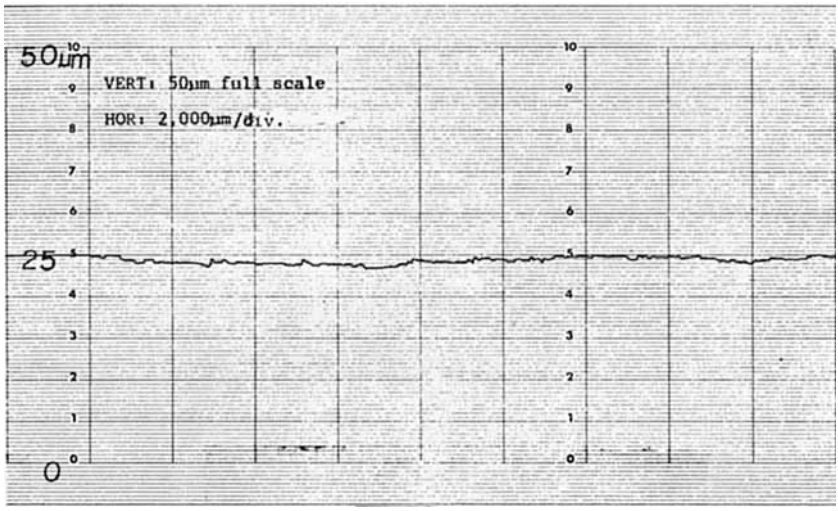

(a)

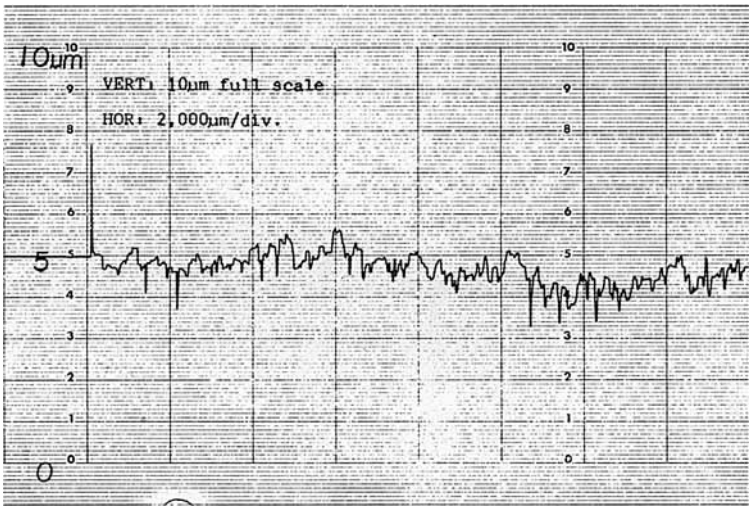

(b)

Fig. 3. Surface profile recording of PAA aluminum.

with hydroxyl ions) probably accounts for the wettability of the surface by water and by adhesive primer, even in the presence of some contamination.

It is known that the columnar structure perpendicular to the aluminum surface has low resistance to damage by shear forces but high resistance to the longitudinal direction of the oxide columns. Therefore, the shear-mode fracture energy of a PAA aluminum–adhesive joint may be sensitive to the degree of penetration; on the other hand, the opening-mode fracture energy will be less sensitive. This was proposed by Schwartz to interpret his data.[21]

If, indeed, the mechanism is valid, we would expect that the shear fracture strength depends greatly on factors which could affect the degree of penetration of adhesives into the porous structure. Such factors include viscosity and surface energetics of adhesives in liquid state, polymerization and crosslinking kinetics,

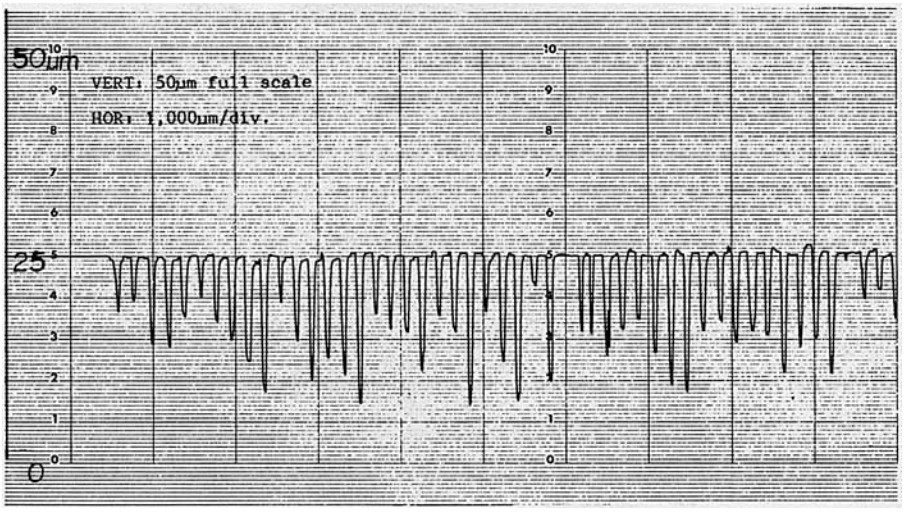

(a)

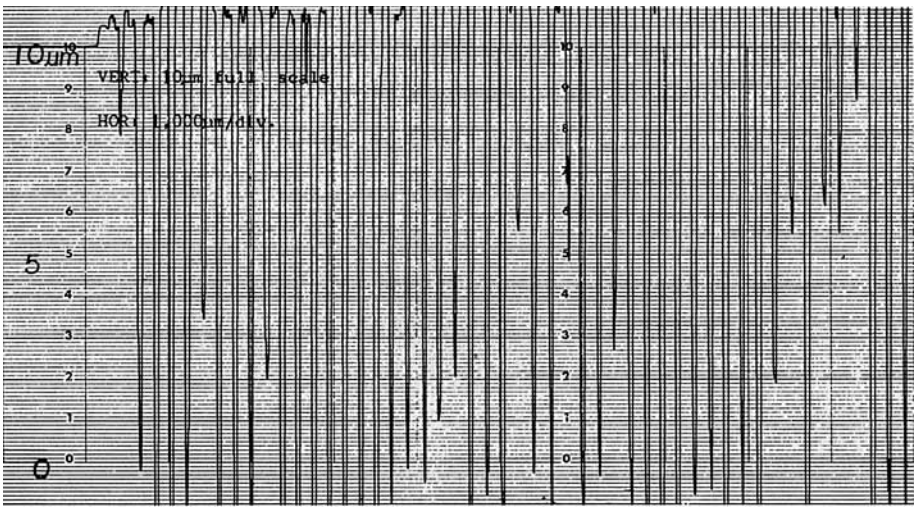

(b)

Fig. 4. Surface profile recording of photolithographically textured aluminum.

volume contraction of adhesive due to crosslinking, temperature of the reaction, amount of gases and vapors trapped in pores, pore size, and pore size distribution. Furthermore, the small size of pores may also interfere with reaction kinetics, change the morphology of the adhesive, and result in a solid adhesive with properties different from its bulk phase. The situation becomes even more

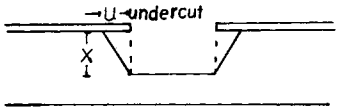

ETCH FACTOR X/U

Fig. 5. Illustration of etch factor.

TABLE I
Effect of Photolithographic Texturing on Bond Strength (Samples 2 × 4 × 0.33 cm, Bond Area 2 × 2 cm, Pull Speed 84.7 μm/sec)

Al 7075T6 condition	Adhesive[a]	Primer	Lap shear strength (6–10 specimens), MPa/psi	Standard deviation, MPa/psi	Failure mode[b]
Degrease only	PL-7293 (177°C Cure)	no	5.89/854	0.41/60	adhesive
Degrease only	PL-7293 (177°C Cure)	PL728	6.83/991	0.54/79	adhesive
PAA and degrease	PL-7293 (177°C Cure)	no	9.69/1405	0.43/63	cohesive
PAA and degrease	PL-7293 (177°C Cure)	P1728	7.12/1032	0.59/86	—
Textured and degrease	PL-7293 (177°C Cure)	no	13.62/1975	0.73/106	cohesive
Textured and degrease	PL-7293 (177°C Cure)	P1728	7.79/1130	0.36/53	cohesive
degrease only	FM1232 (121°C Cure)	no	7.10/1030	0.72/104	adhesive
degrease only	FM1232 (121°C Cure)	BR127	3.76/546	0.22/32	adhesive
PAA and degrease	FM1232 (121°C Cure)	no	15.25/2212	0.86/125	cohesive
PAA and degrease	FM1232 (121°C Cure)	BR127	14.20/2060	0.66/95	cohesive
Textured and degrease	FM1232 (121°C Cure)	no	15.34/2225	0.24/35	cohesive
Textured and degrease	FM1232 (121°C Cure)	BR127	16.17/2345	1/145	cohesive

[a] FM1232 and BR127 were supplied by the American Cynamid Co.; PL729-3 and PL728 were supplied by the BFGoodrich Co.
[b] Visual observation.

TABLE II
Effect of Applied Pressure During Curing on Bond Strength

A17075T6 Condition	Adhesive	Primer	Pressure during curing, MPa	Lap shear strength, MPa/psi	Standard deviation, MPa/psi
Degrease	PL7293 (177°C cure)	PL-728	<0.0345	6.83/991	0.54/79
	PL7293 (177°C cure)	PL-728	0.6895	9.24/1340	0.34/49
PAA and degrease	PL7293 (177°C cure)	PL-728	<0.0345	7.12/1032	0.59/86
	PL7293 (177°C cure)	PL-728	0.6895	10.76/1560	0.19/28
Textured and degrease	PL7293 (177°C cure)	PL-728	<0.0345	7.79/1130	0.36/53
	PL7293 (177°C cure)	PL-728	0.345	10.96/1590	0.19/28
Textured and degrease	FM-1232 (121°C cure)	BR-127	<0.0345	16.17/2345	1/145
	FM-1232 (121°C cure)	BR-127	0.345	16.83/2442	0.43/62

TABLE III
Effect of Immersion in Water for 100 Days on Bond Strength

A17075T6	Adhesive	Primer	Water immersion	Lap shear strength, MPa/psi	Standard deviation, MPa/psi
Degrease only	PL-7293 (177°C cure)	PL-728	no	6.83/991	0.54/79
Degrease only	PL-7293 (177°C cure)	PL-728	yes	5.14/745	0.51/74
PAA and Degrease	PL-7293 (177°C cure)	PL-728	no	7.12/1032	0.59/86
PAA and Degrease	PL-7293 (177°C cure)	PL-728	yes	10.8/1563	0.68/98
Textured and degrease	PL-7293 (177°C cure)	PL-728	no	13.6/1975	0.73/106
Textured and degrease	PL-7293 (177°C cure)	PL-728	yes	9.05/1313	0.59/85
Degrease only	FM-1232 (121°C cure)	BR127	no	6.83/991	0.54/79
Degrease only	FM-1232 (121°C cure)	BR127	yes	3.45/500	0.97/141
PAA and degrease	FM-1232 (121°C cure)	BR127	no	14.2/2060	0.66/95
PAA and degrease	FM-1232 (121°C cure)	BR127	yes	15.3/2216	0.94/137
Textured and degrease	FM-1232 (121°C cure)	BR127	no	16.2/2345	1/145
Textured and degrease	FM-1232 (121°C cure)	BR127	yes	6.38/925	0.91/132

TABLE IV
Surface Properties of Aluminum Samples

Sample	History	Ellipsometry Δ,[a] deg	Ellipsometry ψ,[b] deg	SPD, Volt	PEE nA	θ H_2O, deg
Al	Degrease only	280	60	0.38	0.15	53
B1	PAA and degrease	177	26	1.0	0.14	71
C2-1	Textured side	113	38	0.40	0.60	66
C2-2	Untextured side	116	39	0.38	0.60	71

[a] The phase shift of light polarized perpendicular to plane of incidence (POI) with respect to that polarized parallel to POI.

[b] The arc tangent to the reflection coefficients for both components.

complex if the applied adhesive is heterogeneous, since not every component is able to penetrate into the porous structure.

It was recognized a long time ago[22,23] that the establishment of a virtual contact equilibrium through penetration may be the process determining the rate at which a bond progresses toward its maximum. However. in recent years, no such study has been done to the best of the authors' knowledge, although many other aspects of adhesion and adhesives have been extensively investigated. This is probably due to the difficulty in preparing surfaces with well-defined and

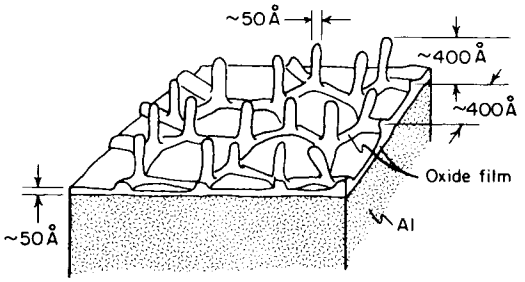

Fig. 6. Isometric drawing of oxide structure on FPL surface.

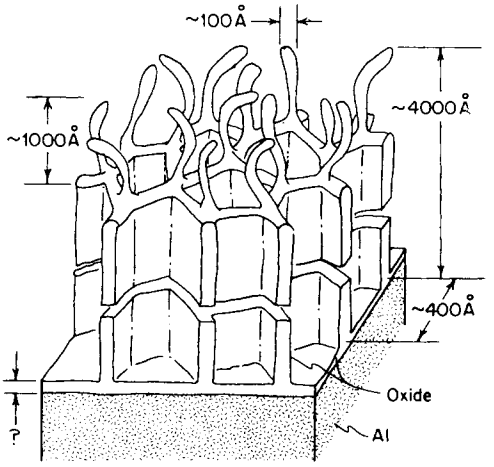

Fig. 7. Isometric drawing of oxide structure on PAA surface.

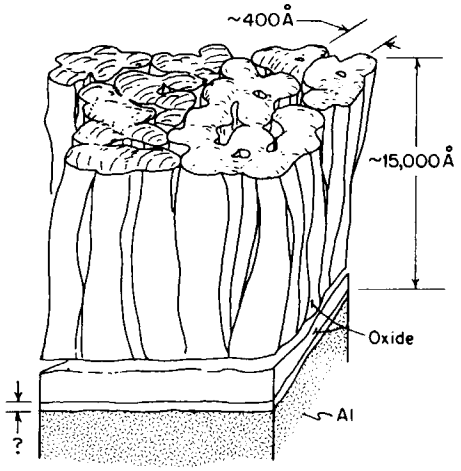

Fig. 8. Isometric drawing of oxide structure on CAA surface.

well-controlled texture. With our photolithographic surface texturing technique, this difficulty will no longer exist.

Several interesting conclusions can be drawn from the tabulated data. The average strength of textured specimen is about 40% higher than that of PAA specimens for the 177°C-cure adhesive without primer. The difference in 121°C-cure adhesive is much less, although the textured specimen is still superior. This suggests that it is more advantageous to prepare the surface with large pores if the adhesive is more viscous. One interesting observation is that the presence of primer greatly reduces the strength of high-temperature adhesives. This is not inconsistent with the findings of Schwartz.[21] His data showed that for the 7075–T6/PL 729 system, the crack extension rate of the unprimed specimens was smaller than that of primed ones at 60°C and 95% relative humidity. This could be due to either one or more of the following factors: poor wetting characteristic, high viscosity, or overcure of the primer.

As shown in Table II, increasing the applied pressure during curing not only increases the average joint strength (predominantly shear) but also reduces its standard deviation, a very interesting observation. Increase in pressure seems to have a much stronger effect on 177°C cure adhesives than the 121°C cure adhesives. We intend to qualitatively interpret our data in terms of the degree of penetration of adhesives into the holes in the aluminum oxide surface.

Let us first idealize a hole in the surface by a close-ended tube of which the radius is r and the length is L. With reference to Figure 9, by assuming that the wetting angle is 0, we have

$$P_A - P_B = P_A - P_c + \frac{2\sigma}{r} \tag{1}$$

where P_A, P_C, and σ are the press pressure, the pressure of trapped gas in the tube, and the surface tension of the adhesive, respectively. Although the assumption of zero wetting angle may not be valid in practical situations, it should not affect our conclusions, since we are only interested in qualitative interpretations. If the trapped gas follows the ideal gas law, we have

$$P_C = \frac{P_{C0}L}{L - Y} \tag{2}$$

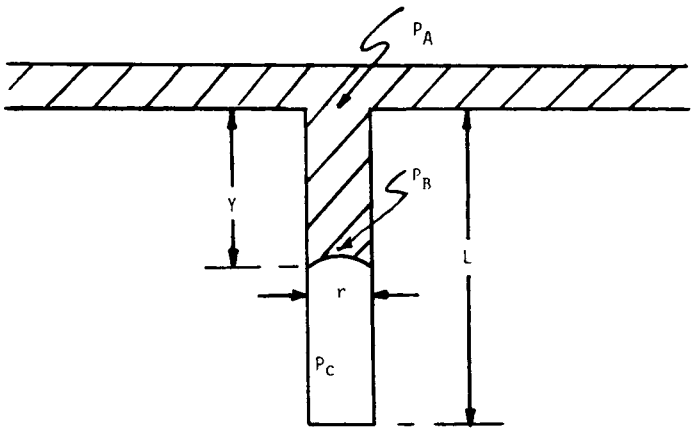

Fig. 9. Penetration of an adhesive into a blind hole.

where Y is the penetration distance of adhesive into the pore and P_{C0} is the gas pressure before the press pressure is applied, i.e., when $Y = 0$. Assuming the flow acts like it is fully developed and in quasi-steady state, the flow rate is given by the Hagen–Poiseuille equation, which for this case becomes

$$\frac{dY}{dt} = \frac{P_A - P_B + \rho g Y}{8\,\mu Y} \tag{3}$$

where t, g, ρ, and μ are time, gravitational acceleration, density, and viscosity of the adhesive, respectively. Solving eq. (3), we obtain

$$t = A\hat{Y} + \frac{AC\hat{L}}{B^2}\frac{\ln \hat{Y} + C/B}{C/B} - A\left(B + \hat{L} + \frac{C\hat{L}}{B^2}\right)\frac{ln(\hat{Y} + B - C/B)}{B - C/B} \tag{4}$$

where

$$A = \frac{8\mu}{\rho g r} \tag{5}$$

$$B = -\hat{L} + \frac{2\sigma}{\rho g r^2} + \frac{p}{\rho g r} \tag{6}$$

$$C = \frac{-\hat{L}(P_A - P_{C0})}{(\rho g r) - 2\sigma\hat{L}/(\rho g r^2)} \tag{7}$$

$$\hat{Y} = \frac{Y}{r} \tag{8}$$

$$\hat{L} = \frac{L}{r} \tag{9}$$

In deriving eq. (4), we assume $B^2 \gg 4C$, which is a very realistic approximation as will be shown.

In order to apply eq. (4) to interpret our experimental results, we assume that $\mu = 10^2$ Pa·s (10^3 poise), $\rho = 10^3$ kg/m^3, and $\sigma = 5 \times 10^{-2}$ N/m. As we already have shown in Figures 1, 4, and 7, a typical value of r is 20 nm for the PAA surface and 20 μm for the textured surface, and L is 400 nm and 10 μm for the PAA and the textured surface, respectively.

Consider two cases, one with a $P_A - P_{C0}$ of 0.03 MPa (we call it low pressure) and the other with a $P_A - P_{C0}$ of 1 MPa (we call it high pressure). The maximal penetration of $\hat{Y}$ as given by eq. (4) is $-C/B$, which is $0.98\hat{L}$ for the PAA surface and $0.334\hat{L}$ for the textured surface at low pressure. With an increase in applied pressure to 1 MPa, the maximal penetration of $\hat{Y}$ increases to $0.995\hat{L}$ and $0.994\hat{L}$ for PAA surface and textured surface, respectively. Apparently, at low pressure, the total available contact area within a hole, which is proportional to L, is not fully utilized for the texture surface. However, at high pressure, the theoretical maximal penetration for both surfaces is acceptable.

This discussion cannot be complete without addressing ourselves to the question of rate of penetration. Obviously, to reach the theoretical maximal penetration, an infinitely long time is needed; however, to reach a penetration reasonably close to the maximal value may require only a very short time. For the PAA surface a penetration of $0.95\hat{L}$ requires only 0.031 sec at low pressure and 0.023 sec at high pressure. For the textured surface, a penetration of $0.333\hat{L}$ requires 2.3×10^{-3} sec at low pressure and a penetration of $0.95\hat{L}$ requires 9×10^{-3} sec. Therefore, we conclude that for all practical purposes, the rate of penetration is fast enough and shall not cause any concern.

If one accepts the concept that the degree of penetration dictates the joint strength, the above theoretical results agree with the experimental fact that an increase in pressure improves the strength of joints. However, it fails to explain why the textured surface has even a higher strength than the PAA surface, especially for the 177°C-cure adhesive. The experimental fact seems to suggest that the enormous high surface area provided by the PAA treated surface was not fully exploited. Why? To answer this question, we have to examine Figure 3 again. As shown there, the PAA surface is very irregular, with many large spikes and pits the height or depth of which is in the order of 1 μm and a base on window opening is in the order of 10 to 100 μm. The fine-scale holes as shown in Figure 7 are sitting on top of these large-scale spikes or pits. It is the large-scale roughness which controls the maximal degree of penetration. If the adhesive is able to fully penetrate these large-scale pits, then, according to our analysis, it would have no problem in penetrating the small holes. At low pressure, the air trapped in these large shallow pits in the PAA surface resists the penetration. For high-temperature adhesive, we suspect that the vapor pressure of the solvent may increase P_C and hence make the penetration more difficult.

Another striking result is the poor performance of textured specimens after immersion in water for 100 days, in contrast with the gain in strength for the PAA specimens after a similar immersion (Table IV). It is true that from the adhesion, point of view, an interfacial property, water should only have a detrimental effect. Therefore, we suspect that this seemingly unbelievable observation might result from something other than those of interfacial origin. It is possible that during the time of water immersion, chemical reactions continued in the adhesive layer, which resulted in changes of mechanical properties of adhesive and shrinkage strain. These changes, in turn, caused a redistribution of stress concentration near the adhesive–adherend interface. Since the surface profiles of PAA specimens and that of textured specimens are very different, it is not unreasonable to have different effects. However, we could not verify this argument at the present time.

The ellipsometric Δ, ψ values for the degreased sample aluminum do not confirm to any theoretical oxide thickness values. The PAA sample has surface properties in close agreement with many such samples that were produced by Rockwell International Science Center, except ψ, which is about 10° low. The hydroxide film of PAA sample is estimated above 3000 Å from the Δ value.[18] The textured and nontextured sides have about the same properties, since the tools used are not sensitive to the large dimensions of the pit array. The oxide film is estimated to be about 300 Å. The large difference of surface potential difference and photoelectron emission between the PAA sample and the textured sample suggests that the surface chemical properties of these two are very different. A more detailed study is needed before the exact meaning can be understood. We intend to address to this question in a later publication. The contact angles for water indicates all the samples are contaminated with organic substances. However, this result might be misleading, since this measurement was conducted many days after the surface of specimens was degreased. We do not believe that aluminum plates used for preparing lap joints were that badly contaminated.

In conclusion, we introduce an interesting new technique to control the surface profile of an adherend. Preliminary data and model analysis suggest that the degree of contact dictates the shear strength of joints. Moreover, it shows that the new technique could render a stronger bond than the conventional PAA technique. However, the effect of degree of contact on the adhesive joint strength is to some extent blurred by the possible differences in surface energetics between PAA and photoetched specimens. The surface chemical properties of the latter can be modified by selecting different etchants. Certainly more work is needed before a definite picture can be drawn. However, the new technique does provide a tool and a rational scheme to understand the effect of surface profile on the adhesive joint strength.

This project was partially supported by a Ford Company Research Initiation grant made available through the Engineering School, University of Southern California. We like to express our gratitude to Dr. M. A. Danforth of McDonnell Douglas Corporation for kindly sending us the PAA panels, Dr. T. Smith for conducting the surface chemical studies, BFGoodrich Company and American Cynamid Company for sending the adhesives, Professors N. W. Tschoegl and W. G. Knauss for allowing us to use their Instron machines, Dr. H. Y. Hsu and Mr. N. Kuo for conducting the mechanical tests.

References

1. A. Brief and I. Skeist, in *Applied Polymer Science*, J. K. Craver and R. W. Tess, Am. Chem. Soc., Washington, D.C., 1975, Chap. 33.

2. A. N. Gent, Ed., *The Relation of Molecular Structure to Adhesion*, a Report on a Research Workshop sponsored by AFOSR, held at the University of Akron, Akron, OH, May 29–30, 1979.

3. N. Moskvitin, *Physico-chemical Principles of Gluing and Adhesion Processes*, U.S. Dept. of Commerce, Clearing House or Federal Scientific and Technical Information, Springfield, VA, 1969.

4. B. V. Derjaguin and V. P. Smilga, in *Adhesion*, D. D. Eley, Ed., Oxford Univ. Press, London, 1961, Part III, Chap. 6.

5. S. S. Voyutskii, *Adhesive Age*, **5**, 30 (1962).

6. F. M. Fowkes and M. A. Mostafa, *Ind. Eng. Chem. Prod. Res. Dev.*, **17**, 3 (1978).

7. D. H. Kaelble, *J. Appl. Polym. Sci.*, **18**, 1869 (1974).

8. D. H. Kaelble, P. J. Dynes, and D. Pav, in *Adhesion Science and Technology*, Vol. 9B, L. H. Lee, Ed., Plenum, New York, 1975, p. 735.

9. (a) K. L. Mittal, in *Adhesion Science and Technology*, Vol. 9A, L. H. Lee, Ed., Plenum, New York, 1975, p. 129; (b) K. L. Mittal, *Polym. Eng. Sci.*, **17**, 463 (1977).

10. J. J. Bikerman, *The Science of Adhesive Joints*, Academic New York, 1968.

11. H. Schonhorn, in *Adhesion*, D. D. Eley, Ed., Oxford University Press, London, 1961, Part I, Chap. 3, p. 12.

12. G. R. Irwin, in *Treatise on Adhesion and Adhesives*, Vol. 1, R. L. Patrick, Ed., Marcel Dekker, New York, 1967, Chap. 7.

13. M. L. Williams, *J. Adhesion*, **4**, 307 (1972).

14. G. Salomon, in *Adhesion and Adhesives*, R. Houwink and G. Salomon, Eds., Elsevier, New York, 1965, Chap. 1.

15. W. A. Zisman, in *Contact Angle, Wettability and Adhesion*, R. F. Gould, Ed., Adv. Chem. Ser., Vol. 43, Am. Chem. Soc., Washington, D.C., 1964, p. 1.

16. J. F. Oliver and S. G. Mason, *J. Colloid Interfac. Sci.*, **60**, 480 (1977).

17. K. L. Mittal, *Solid State Technology* (May 1979), pp. 89–95.

18. T. Smith, Non-Destructive Inspection of PAA Aluminum Panels for Contamination, AFML-TR-74-74, Part II, August, 1975; in *Surface Contamination: Genesis, Detection and Control*, Vol. 2, K. L. Mittal, Plenum, New York, 1979, pp. 697–713.

19. P. F. A. Bijlmer, see Ref. 18, pp. 723–748.

20. M. A. Danforth and R. J. Sunderland, *Proceedings of Symposium on Durability of Adhesive Bonded Structures*, Picatinny Arsenal, October 1976, p. 303.

21. H. S. Schwartz, see Ref. 20, p. 101.

22. N. A. de Bruyne, *Aero Research Technical Notes No. 168*, Duxford, 1956.

23. W. C. Wake, in *Adhesion*, D. D. Eley, Ed., Oxford University Press, London, 1961, p. 111.

Received February 18, 1980
Accepted November 26, 1980